

## RESEARCH ARTICLE

# Of flippers and wings: The locomotor environment as a driver of the evolution of forelimb morphological diversity in mammals

Priscila S. Rothier<sup>1,2</sup>  | Anne-Claire Fabre<sup>3,4,5</sup>  | Roger B. J. Benson<sup>6,7</sup>  |  
 Quentin Martinez<sup>8,9</sup>  | Pierre-Henri Fabre<sup>8,10</sup>  | Brandon P. Hedrick<sup>2</sup>  |  
 Anthony Herrel<sup>1,3,11,12</sup> 

<sup>1</sup>Département Adaptations du Vivant, Muséum National d'Histoire Naturelle, Paris, France; <sup>2</sup>Department of Biomedical Sciences, College of Veterinary Medicine, Cornell University, Ithaca, New York, USA; <sup>3</sup>Naturhistorisches Museum Bern, Bern, Switzerland; <sup>4</sup>Institute of Ecology and Evolution, University of Bern, Bern, Switzerland; <sup>5</sup>Life Sciences Department, Vertebrates Division, Natural History Museum, London, UK; <sup>6</sup>American Museum of Natural History, New York, New York, USA; <sup>7</sup>Department of Earth Sciences, University of Oxford, Oxford, UK; <sup>8</sup>Institut des Sciences de l'Évolution de Montpellier, Université de Montpellier, Montpellier, France; <sup>9</sup>Staatliches Museum für Naturkunde Stuttgart, Stuttgart, Germany; <sup>10</sup>Institut Universitaire de France (IUF), Paris, France; <sup>11</sup>Department of Biology, Evolutionary Morphology of Vertebrates, Ghent University, Ghent, Belgium and <sup>12</sup>Department of Biology, University of Antwerp, Wilrijk, Belgium

## Correspondence

Priscila S. Rothier

Email: [pd425@cornell.edu](mailto:pd425@cornell.edu)

## Funding information

Conselho Nacional de Desenvolvimento Científico e Tecnológico, Grant/Award Number: 204841/2018-6; Synthesis of Systematic Resources (SYNTHESES) Project, by the European Community Research Infrastructure Action; European Commission, Grant/Award Number: GB-TAF-5737, GB-TAF-6945 and GB-TAF-1316; Agence Nationale de la Recherche, Grant/Award Number: ANR-17-CE02-0005 RHINOGRAD 2017; European Research Council, Grant/Award Number: ERC-2015-STG-677774; National Science Foundation (NSF), Grant/Award Number: DBI-1701713, 1701714, 1701737, 1702263, 1701665, 1701767, 1701769, 1701870, 1701797, 701851, 1702442, 1902105, 1902242, DEB-9873663, BCS 1317525, BCS 1540421 and BCS 1552848; Leakey Foundation

Handling Editor: Kris Crandell

## Abstract

1. The early diversification of tetrapods into terrestrial environments involved adaptations of their locomotor apparatus that allowed for weight support and propulsion on heterogeneous surfaces. Many lineages subsequently returned to the water, while others conquered the aerial environment, further diversifying under the physical constraints of locomoting through continuous fluid media. While many studies have explored the relationship between locomotion in continuous fluids and body mass, none have focused on how continuous fluid media have impacted the macroevolutionary patterns of limb shape diversity.
2. We investigated whether mammals that left terrestrial environments to use air and water as their main locomotor environment experienced constraints on the morphological evolution of their forelimb, assessing their degree of morphological disparity and convergence. We gathered a comprehensive sample of more than 800 species that cover the extant family-level diversity of mammals, using linear measurements of the forelimb skeleton to determine its shape and size.
3. Among mammals, fully aquatic groups have the most disparate forelimb shapes, possibly due to the many different functional roles performed by flippers or the relaxation of constraints on within-flipper bone proportions. Air-based locomotion, in contrast, is linked to restricted forelimb shape diversity. Bats and gliding mammals exhibit similar morphological patterns that have resulted in partial phenotypic convergence, mostly involving the elongation of the proximal forelimb segments.

This is an open access article under the terms of the [Creative Commons Attribution](https://creativecommons.org/licenses/by/4.0/) License, which permits use, distribution and reproduction in any medium, provided the original work is properly cited.

© 2024 The Author(s). *Functional Ecology* published by John Wiley & Sons Ltd on behalf of British Ecological Society.

4. Thus, whereas aquatic locomotion drives forelimb shape diversification, aerial locomotion constrains forelimb diversity. These results demonstrate that locomotion in continuous fluid media can either facilitate or limit morphological diversity and more broadly that locomotor environments have fostered the morphological and functional evolution of mammalian forelimbs.

#### KEYWORDS

disparity, macroevolution, osteology, phenotypic convergence

## 1 | INTRODUCTION

Phenotypic evolution is in part dictated by the physical properties of the environment that surrounds living organisms (Vogel, 2020). Particularly, the different substrates used by animals for locomotion, such as land, air and water, differ in density and viscosity, impacting the capacity of animals to move (Biewener & Patek, 2018). With the rise of Tetrapoda and the evolutionary transition from water to land, a series of morphophysiological modifications were critical for organisms to support their body weight against gravity on heterogeneous terrestrial surfaces in addition to providing propulsion. Most notably, locomotor adaptations involved the evolution of three-segmented limbs with distal hands and feet that accommodate the substrate surface and provide thrust to propel the organism on land (Shubin et al., 1997), which later diversified into distinct morphological and locomotor specialisations for navigating terrestrial ecosystems in novel ways (such as adaptations for cursoriality, arboreality, fossoriality, climbing, jumping, bipedalism and graviportality, among others, Polly, 2007). As tetrapods successfully radiated across the globe, some lineages independently returned to water and others conquered the aerial realm, both experiencing constraints on locomotion imposed by moving in continuous fluid media (Vogel, 2020).

Although locomotion in water and air consists of moving through continuous fluids, the differences in density between these two media constrain locomotor biomechanics in different ways (Biewener & Patek, 2018). Whereas the main challenge of underwater locomotion is to overcome drag in a dense and viscous fluid, the weaker buoyancy and lower density of air require animals to generate sufficient lift and provide mechanical power to traverse their environment (Biewener & Patek, 2018; Rayner, 1988). Such fundamental differences between media have long been suggested to differentially impact the morphological evolution of lineages that locomote in these environments (Fish et al., 2008; Gutarra et al., 2022; Gutarra & Rahman, 2022; Norberg, 1985), potentially limiting trait diversity and driving distinct patterns of phenotypic similarity.

Studies on macroevolution have most often examined the relationship between body mass and ecological adaptations associated with moving through different media (Benson et al., 2018; Burin et al., 2023; Godoy et al., 2019; Pyenson & Vermeij, 2016). Aquatic lineages tend to rapidly evolve large body mass, while aerial taxa are generally confined to relatively small body masses (Burin et al., 2023; Dudley et al., 2007; Gearty et al., 2018; Kiat et al., 2021). Increases

in body mass associated with moving into fully aquatic niches are likely driven by the energetic balance between heat loss and feeding efficiency dictated by prey availability (Gearty et al., 2018; Gutarra et al., 2022; Pyenson & Vermeij, 2016; Smith & Lyons, 2011). Unlike swimming, aerial locomotion faces significant constraints related to body weight support. A lighter body mass may reduce the energetic cost of flight and improve aerial manoeuvrability in volant organisms (Gatesy & Middleton, 2007; Rayner, 1988), resulting in gliding and flying animals having an upper limit to body mass (Dudley et al., 2007). Alongside body mass, limb morphology also appears to be influenced by the locomotor environment, yet the comprehensive comparative analyses needed to test this hypothesis are lacking.

While underwater, limbs no longer provide weight support. Forelimbs in aquatic taxa often become proportionally short (Maher et al., 2022), either functioning to provide thrust and/or assist in controlling swimming stability and manoeuvrability (Gutarra & Rahman, 2022). Within-limb joint mobility is usually very restricted, including loss of arm-twisting, often accompanied by a modification of the limb into paddle-like flippers (Cooper, Dawson, et al., 2007; Motani & Vermeij, 2021). In turn, volant lineages present proportionally longer overall forelimb lengths compared to almost all other tetrapod lineages (Maher et al., 2022). In mammals, all flying and gliding species have a patagium, a membranous skin extension stretched laterally to the body and to the forelimbs that increases lift and slows acceleration during descent (Bishop, 2008; Dudley et al., 2007). Forelimb elongation grants an increase in the surface area for the attached patagia, facilitating lift generation (Gatesy & Middleton, 2007; Grossnickle et al., 2020). Although many similarities are observed within lineages that independently left land to move in the same fluid medium, it remains unclear whether biomechanical properties of continuous fluids act to constrain the evolution of limb shape diversity or not.

Mammals are an ecologically and morphologically diverse group, displaying remarkable locomotor diversity adapted to different environments, making them an excellent group to evaluate how the locomotor environment impacts forelimb morphology (Chen & Wilson, 2015; Polly, 2007). Most mammals use the terrestrial locomotor environment (e.g. the ground, trees, etc.) to move across the landscape. However, their evolutionary history is marked by transitions from locomotion on land to both aquatic and aerial locomotion, as well as the interface of these media with terrestrial surfaces (Figure 1; Nowak, 1999). Here, we ask whether and how long-distance locomotion in these different locomotor environments,

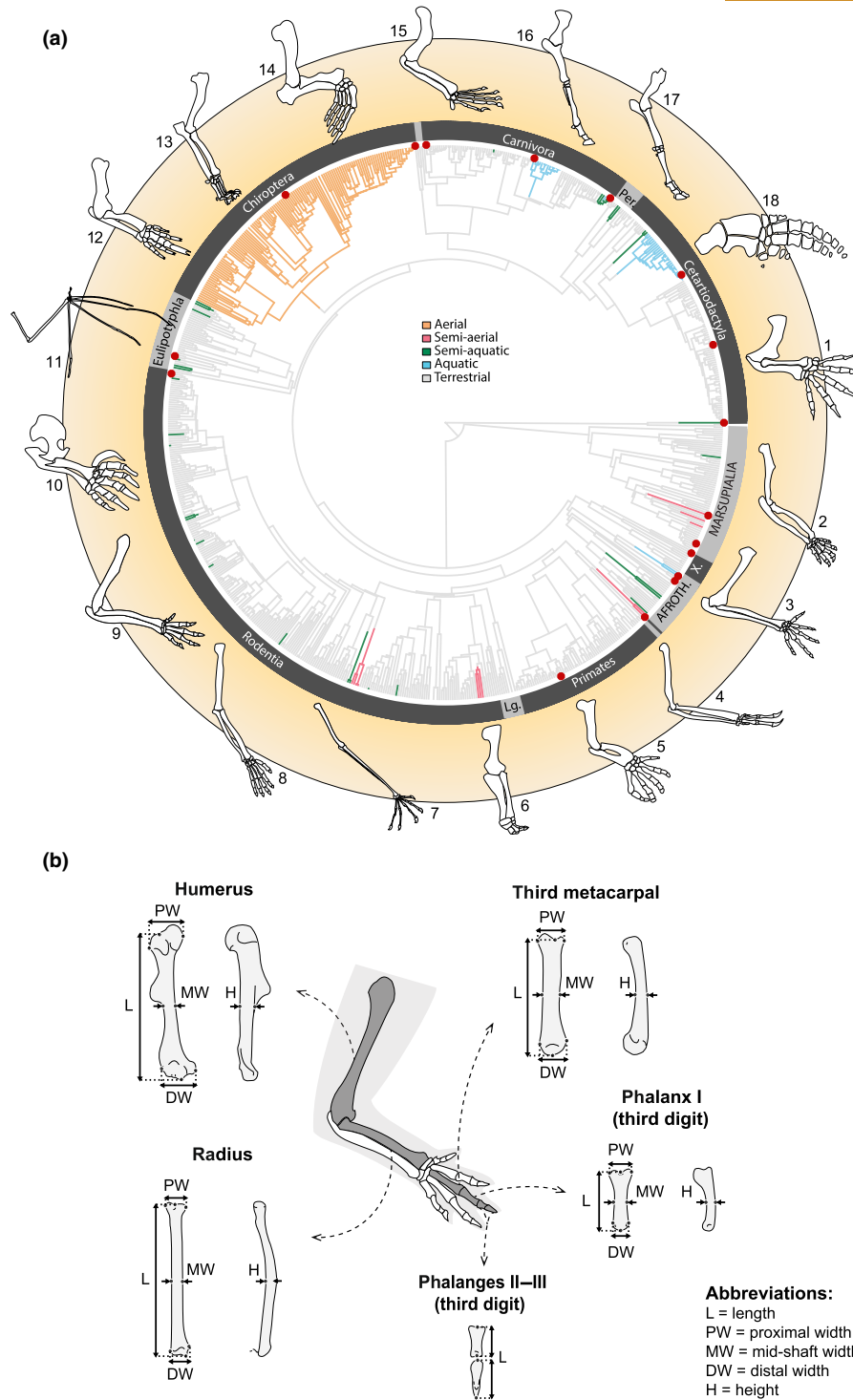


**FIGURE 1** Studies species and examined linear distances. (a) Coloured branches indicate the primary locomotor environment used for locomotion per species. Topology pruned from Upham et al. (2019). Tips labelled with red circles indicate species which forelimb morphology is represented in the image. (1) *Ornithorhynchus anatinus* (Monotremata, Ornithorhynchidae—semi-aquatic); (2) *Macropus giganteus*\* (Diprotodontia, Macropodidae—terrestrial); (3) *Acrobates pygmaeus* (Diprotodontia, Acrobatidae—semi-aerial); (4) *Choloepus didactylus*\* (Pilosa, Megalonychidae—terrestrial); (5) *Trichechus senegalensis* (Sirenia, Trichechidae—aquatic); (6) *Elephas maximus*\* (Proboscidea, Elephantidae—terrestrial); (7) *Galeopterus variegatus* (Dermoptera, Cynocephalidae—semi-aerial); (8) *Homo sapiens*\* (Primates, Hominidae—terrestrial); (9) *Melanomys caliginosus*\* (Rodentia, Cricetidae—terrestrial); (10) *Mogera wogura* (Eulipotyphla, Talpidae—terrestrial); (11) *Barbastella barbastellus* (Chiroptera, Vespertilionidae—aerial); (12) *Manis pentadactyla*\* (Pholidota, Manidae—terrestrial); (13) *Panthera leo*\* (Carnivora, Felidae—terrestrial); (14) *Odobenus rosmarus* (Carnivora, Odobenidae—aquatic); (15) *Lutra lutra* (Carnivora, Mustelidae—semi-aquatic); (16) *Equus caballus*\* (Perissodactyla, Equidae—terrestrial); (17) *Bos frontalis*\* (Cetartiodactyla, Bovidae—terrestrial); (18) *Tursiops truncatus*\* (Cetartiodactyla, Delphinidae—aquatic). \* Limb schemes modified from Rotherier et al., 2023. (b) Representation of the studied bones and the obtained morphological distances.

terrestrial, aquatic, aerial, and at their interface, impacts the morphological diversity of the forelimb skeleton, determining the patterns of skeletal shape diversity as well as changes in absolute forelimb size. We investigate patterns of phenotypic variation, disparity, and convergence using a comparative framework based on a comprehensive sample of more than 800 species of mammals, capturing nearly all family-level diversity of extant mammalian species. We predict that the use of homogeneous fluids, such as water and air, will result in less disparate phenotypes, reflecting convergent locomotor adaptations that overcome the physical constraints imposed by locomotion in continuous fluids.

## 2 | METHODS

### 2.1 | Taxonomic sample and morphological inference

Our dataset consists of forelimb dimensions from 837 species (796 genera and 153 families capturing over 60% of mammal genus diversity and more than 90% of modern and recently extinct mammalian families, Mammal Diversity Database, 2023) using 874 specimens (Table S1), representing most living mammalian orders (all orders except for the marsupial moles *Notoryctemorphia*, which have fused digit bones that prevented taking of the measurements used here). Our study comprises an extended sample relative to Rothier et al. (2023), with 199 additional species. Each species was represented by one to three individuals. Unfortunately, we were unable to account for sex variation, as this information was most often unavailable for the studied specimens. Data acquisition was conducted by combining digital and manual methods, depending on the specimen's size. We generated microCT scans and surface scans of 132 small to medium-sized specimens from different institutions. Scans were generated using a Nikon Metrology HMX ST 225 (NHMUK Natural History Museum, London) and an EasyTom 150 X-ray microcomputer tomography (ISEM Institute, Montpellier, France). Additionally, we included 414 meshes downloaded from MorphoSource.org. We used Avizo 8.1.1 (1995–2014 Zuse Institute Berlin) to convert image stacks into three-dimensional surface models (incorporating scale dimensions based on the voxel size of each scan) later used to obtain morphometric distances via landmark coordinates (Figure 1), also in Avizo. Finally, we took calliper measurements from 328 limb skeletons of medium to large body sized species available at the Muséum National d'Histoire Naturelle (MNHN Paris, France), the American Museum of Natural History (AMNH New York, USA), and the Natural History Museum (NHM London, UK; Table S1).

To capture forelimb morphology, we used 21 linear distances on the bones of the forelimb, following the measurements described by Rothier et al. (2023). The distances consisted of the length, width (proximal, medial and distal axis) and height of the humerus, radius, third metacarpal and first phalanx of digit III, in addition to the total length of the digit III, inferred as the sum of, the lengths of all phalanges of digit III (see Figure 1 and Table S2 for data description). We did not include the ulna because this bone is fused to the radius in

many taxa (e.g. Chiroptera and Equidae; Sears et al., 2007), preventing measurement.

We chose to sample the third finger because this is the only digit present in the hands of all mammalian species, even in groups that exhibit digit loss or fusion with other autopodial elements (Clifford, 2010; McHorse et al., 2019; Prothero, 2009). We measured each individual twice with the subsequent calculation of the mean and standard error to assess measurement error. Error estimates were generally below 1.5% regardless of the size of the animal and the measurement method, indicating the reliability and repeatability of the methods employed. Body mass information was rarely available for the analysed specimens, so we extracted body mass estimates per species from the PanTHERIA database (Jones et al., 2009) and from complementary literature sources when necessary (Table S1).

### 2.2 | Classification of locomotor environment

We classified species based on their main locomotor environment, interpreted as the different physical media mostly used for travel: terrestrial (607 species), aquatic (53 species), semi-aquatic (39 species), aerial (bats only, 127 species) and semi-aerial (11 species). We considered 'terrestrial' as the medium for locomotion of all species that actively move and travel on land, including cursorial, arboreal, saltatorial, striding and fossorial mammals (following Nowak, 1999). Species classified in the 'aquatic' category are completely dependent on water and present minimised land travel and loss of terrestrial feeding (Motani & Vermeij, 2021). The aquatic category includes all cetaceans, pinnipeds, sirenians and the sea otter *Enhydra lutris* (Howell, 1970; Motani & Vermeij, 2021; Nowak, 1999). The only taxa included in the "aerial" category were in the Order Chiroptera, the sole mammal group capable of powered flight. We also included semi-aquatic and semi-aerial species as separate classifications, which groups mammals that combine land-based substrates and fluid media for locomotion. 'Semi-aquatic' ranges from water rats to hippopotami, efficiently move both underwater and on terrestrial substrates but are highly dependent on the aquatic environment for foraging (classification based on DeBlois & Motani, 2019; Motani & Vermeij, 2021; Nowak, 1999; Vermeij & Motani, 2018). 'Semi-aerial' incorporated the gliding mammals which are also active arboreal climbers bearing a patagium (following Jackson, 2000; Nowak, 1999).

### 2.3 | Replication statement

Scale of inference	Scale at which the factor of interest is applied	Number of replicates at the appropriate scale
Species	Species	607 terrestrial species, 53 aquatic species, 39 semi-aquatic species, 127 aerial species and 11 semi-aerial species.

## 2.4 | Comparative framework and datasets

Analyses were implemented in R v. 4.3.1 (R Core Team, 2023). We estimated a maximum clade credibility (MCC) tree from a posterior sample of 10,000 trees published by Upham et al. (2019), using the phangorn R package v 2.11.1 (Schliep, 2011). We analysed our data using two complementary approaches, first pooling all the distances acquired from all bones as a proxy for whole forelimb morphology, and then by analysing each bone individually. We separated the database into two subsets, the first one comprising all measurements, and the second one excluding digit length. Sample size between subsets was not the same, because total digit length could not be calculated for all specimens given that some of them lacked distal phalanges (frequently kept within the specimen's skin prior to its deposition at zoological collections), resulting in 797 species for analyses with the first subset (whole forelimb morphology) and 837 species for the second one (variation per bone).

## 2.5 | Morphological analyses

All morphological distances were  $\log_{10}$ -transformed prior to analyses. We conducted the analysis first correcting the  $\log_{10}$ -transformed measurements for body size (referred as shape or size residual data) and then using these values without size correction (referred as size or raw data). To account for the effects of body size on forelimb morphology, we calculated the geometric means of each species as a proxy for body size. The geometric means were calculated from (1) the species body mass transformed into the linear scale (by taking the cube root prior to  $\log_{10}$ -transformation, Harmon et al., 2010), and (2) the species forelimb distances, repeating this procedure for both subsets. We then regressed the  $\log_{10}$ -transformed distance measurements on the geometric mean overall size using phylogenetic generalised least squares (PGLS with `mvglis()` function; `mvMORPH` R package v 1.1.7, (Clavel et al., 2015, 2019)), using the residual distance measurements as a proxy for forelimb shape (Rothier et al., 2023). We conducted this procedure with all measurements (first subset) and with each bone individually (second subset). Linear regressions were replicated with LASSO penalisation using the following models of trait evolution: Brownian Motion (BM), Ornstein-Uhlenbeck (OU) and Early Burst (EB). Model fit likelihood was evaluated with the generalised information criterion (GIC). The OU process had the best fit for the size residual data and was in the subsequent analyses (Table S3). We repeated the linear regressions with model fit without geometric means transformation, that is using the raw  $\log_{10}$ -transformed data without size correction to understand the impact of size on forelimb morphology. The OU model also presented the best support for the raw data.

We verified whether forelimb morphology varied across locomotor media via PGLS followed by multivariate analyses of variance, respectively, using the functions `mvglis()` and `mvglis.manova()` from `mvMORPH` R package (Clavel et al., 2015, 2019), using Pillai as a multivariate test. We used the `pairwise.glh()` function, also from `mvMORPH`, for pairwise comparison across locomotor media of the

fitted generalised linear hypotheses (Clavel et al., 2015; Clavel & Morlon, 2020).

## 2.6 | Morphological variation and ecological disparity

We used the phylogenetic residuals from the best-supported fitted linear models in a phylogenetic principal component analyses (pPCA) with the function `mvglis.pca()` from `mvMORPH` (Clavel et al., 2015, 2019). We also ran a regular PCA using the function `prcomp()` from `stats` v 4.3.1 to compare the effect of the phylogenetic structure across the main axes of variation. To estimate the morphological differences between locomotor categories, we used the first four phylogenetic principal components (pPC) provided from all pPCA in a simulation-based phylogenetic ANOVA with 10,000 simulations and post-hoc comparisons of group means, using Holm-Bonferroni method for p-value adjustment (`phylANOVA()` from `phytools`, Revell, 2012). We chose to use a phylogenetic ANOVA to compare the pPCs because phylogenetic PCA provides residuals and scores in the original phylogenetically dependent species space (Revell, 2009). Therefore, it is recommended to use phylogenetic methods when analysing phylogenetic scores.

Next, we assembled the phylogenetic residuals to calculate disparity across ecological groups. We used the function `custom.subsets()` from the R package `disPRity` v 1.8 to split the data into subsets defined by locomotor media (Guillerme, 2018). To verify data robustness and sensitivity to sample size, we calculated 1000 bootstrap pseudo-replicates with full rarefaction using the function `boot.matrix()`, also from `disPRity` (Guillerme, 2018). Disparity was finally calculated as the sum of variances (function `disPRity()` from `disPRity`, Guillerme, 2018) from a non-rarefied bootstrap pseudoreplicate, a proxy for ellipsoid hyper-volume of the ordinated space (Guillerme et al., 2020). We measured the disparity subset overlap using Bhattacharyya distance with a t-test with Bonferroni correction (function `test.disPRity()` from `disPRity`, Guillerme, 2018; Guillerme et al., 2020).

Fully aquatic groups are represented by four independent lineages, while the fully aerial category is solely represented by the monophyletic order Chiroptera. Therefore, we lack statistical power to determine whether the disparity patterns detected for the aerial category is explained by shared ancestry or functional requirements. To address these concerns, we also assessed forelimb disparity within other two fully aquatic monophyletic groups: Cetacea (33 sampled species) and Pinnipedia (17 sampled species). Hence, we can better assess whether forelimb disparities in monophyletic aquatic clades exhibit similarities or differences compared to the monophyletic aerial group. We could not calculate forelimb disparity for the other two monophyletic aquatic groups (Sirenia ( $n=2$ ) and the sea otter *Enhydra lutris* ( $n=1$ )) due to the reduced taxonomic diversity sampled for each lineage. The same reasoning applies for disparity within semi-aerial (six independent families, sample range of 1–3 species sampled per family) and semi-aquatic clades (16 families, maximum of four species per clade).

## 2.7 | Phenotypic convergence

We used the phylogenetic residuals to calculate morphological convergence between ecological categories. We employed the function `search.conv()` from `RRPhylo` v 2.8.0, which tests whether phenotypes of distantly-related clades are more similar to each other than expected by chance (Castiglione et al., 2019). This method has low Type I and Type II error rates and is very fast to compute, even with large phylogenetic trees, and thus is particularly suitable for our dataset. Morphological convergence calculation was based on phylogenetic ridge regression of the traits, which assigns different evolutionary rates to each branch of the phylogeny (Castiglione et al., 2018, 2019). Because we assessed multivariate data, each species at the tree tips is represented by a phenotypic vector (Castiglione et al., 2019). The degree of phenotypic convergence was then inferred by the significance of the angle  $\theta$  between the phenotypic vectors of the species (as the inverse cosine of the ratio product between the species phenotypic vectors, and the product of vectors sizes), accounting for their phylogenetic distance (Castiglione et al., 2019). Possible  $\theta$  values range from  $0^\circ$  to  $180^\circ$ , with small angles implying similar phenotypes. Phenotypic convergence was explored within each locomotor media category except for 'terrestrial' and 'aerial' since both categories share single ancestry. Additionally, we calculated the angle of morphological convergence between aquatic and semi-aquatic taxa, as well as between aerial and semi-aerial groups.

## 3 | RESULTS

### 3.1 | Limb shape variation differs depending on the locomotor environment

Whole forelimb morphology is significantly different between taxa using different locomotor environments, regardless of whether the effect of overall size is corrected for ( $p < 0.001$ , Table S4, all pairwise comparisons are significant). Morphological differences in shape and overall forelimb size between groups are also detected when each bone is examined individually (Table S4). The non-phylogenetically controlled PCA recovers the same overall pattern of variation revealed by the phylogenetic PCA (Table 1, Tables S5–S7, Figures S1–S5). Therefore, we focus on the results obtained from the phylogenetic PCA.

The greatest variation in the whole forelimb shape (shape pPC1 30.1%) relates to the aspect ratio of length versus thickness (Table 1, Figure 2a). Long, slender limb bones (represented by bats, primates, and colugos), are positioned at one extreme of the pPC1 axis and short, thick limb bones are at the other extreme (illustrated by moles, cetaceans, monotremes, and xenarthrans; Figure 2a). Along shape pPC1, phalangeal and metacarpal lengths are the traits with the highest loadings. A phylogenetic ANOVA reveals that the pPC1 scores describing the whole forelimb shape of aerial taxa is significantly different from all other groups (Figure 2c, Table S8). A similar pattern is detected when analysing each bone separately: the proportionally longest humeri and radii are observed in aerial and semi-aerial taxa, while aquatic groups have shorter bones relative to body size (Figure 3a,b, Tables S9 and

S10, Figures S2 and S3). In the autopod, bats stand out from all other groups by having the proportionally longest metacarpals and phalanges (Figure 3c,d, Tables S11 and S12). The phylogenetic scores of whole forelimb shape belonging to the pPC3 (5.5%) and pPC4 (3.73%) do not show a clear association with the locomotor environment (Figure S1, Table S8). For the individual bones, the strongest functional signal is still recovered for the first two phylogenetic principal components, revealing a few significant differences in pPC3 or pPC4. (Figures S2–S5, Tables S9–S12): (1) humerus residual pPC4 (14.15%) differs between aquatic (wide proximal width and narrow mid-shaft width) and semi-aquatic and terrestrial groups; (2) humerus raw pPC4 (1.04%) differs between semi-aquatic (wider proximal width and narrower mid-shaft width) and terrestrial groups; (3) radius raw pPC3 (1.73%) differentiates aquatic (large mid-shaft width and flat height) from all other categories, and (4) metacarpal raw pPC3 (1.56%) differentiates aerial (large proximal width and flat height) from all categories.

As expected, variation in the raw pPC1 of absolute size is largely associated with overall body size, both for the whole forelimb and for each bone (Figures S1–S5). For all pPCA analyses conducted with the raw data, the pPC1 loadings explained more than 90% of the total variance and consistently presented the same signal (Table 1, Figure 2b, Table S6, and Figures S1–S5), with larger animals having the lowest scores. When all pPC1 loadings were negative, we multiplied both loadings and scores by  $-1$  to facilitate the interpretation and visualisation of the results. In other words, larger species, have absolutely larger forelimbs bones than small body sized species.

### 3.2 | Forelimb disparity is influenced by locomotor environment

Morphological disparity in the forelimb was inferred for the shape and size data (with and without size correction). Rarefaction plots demonstrate that an element number (number of species included) equal or higher than five provides a mean disparity value that is very similar to that of the entire dataset, indicating that our findings are robust even with varying sample sizes (Figures S6 and S7). With size correction, aquatic taxa present a significantly higher limb shape disparity than any other ecological group (Figure 4a, Table S13). The same result is obtained for the shape of bones when examined individually except for the metacarpal, for which terrestrial taxa exhibit the highest disparity (Figure 4b–e). Mammal taxa using land-based terrestrial substrates show the second most diverse morphologies after aquatic taxa for the humerus, radius, and phalanx. The aerial taxon presents the lowest whole-limb shape disparity, a pattern that is also detected for the humerus, the radius and the metacarpal. We also calculated disparity across major clades using continuous media and found that cetaceans are the group driving the increase in limb shape variation across aquatic medium users (Figure 5, Table S14). Pinnipeds present the lowest disparity values for the whole limb shape, but bats are the least disparate group when individually considering the shape of the humerus, radius, and phalanx.

Without size correction, the absolute forelimb size disparity is lower in taxa specialised for locomotion in continuous fluids (i.e. swimming

TABLE 1 Phylogenetic principal components describing whole limb morphology.

	Shape (size removed)				Absolute size (raw)			
	pPC1	pPC2	pPC3	pPC4	pPC1	pPC2	pPC3	pPC4
<b>Humerus</b>								
Length	-0.156	-0.271	0.076	-0.084	0.199	0.168	-0.269	0.087
Proximal width	0.078	-0.189	-0.166	-0.141	0.219	-0.064	-0.179	-0.167
Mid-shaft width	0.117	-0.210	-0.315	0.119	0.222	-0.108	-0.210	-0.314
Distal width	0.115	-0.061	-0.230	-0.028	0.219	-0.100	-0.070	-0.206
Height	0.163	-0.305	-0.152	0.191	0.231	-0.147	-0.298	-0.170
<b>Radius</b>								
Length	-0.296	-0.341	0.222	-0.085	0.194	0.305	-0.346	0.236
Proximal width	0.004	-0.122	-0.090	-0.145	0.224	0.004	-0.118	-0.098
Mid-shaft width	0.021	-0.295	0.022	0.014	0.230	-0.013	-0.296	-0.013
Distal width	0.020	-0.095	-0.016	-0.081	0.232	-0.014	-0.101	-0.022
Height	0.049	-0.105	-0.185	0.328	0.222	-0.040	-0.113	-0.195
<b>Metacarpal</b>								
Length	-0.493	-0.057	0.498	-0.063	0.192	0.499	-0.079	0.497
Proximal width	0.124	0.201	0.213	-0.243	0.232	-0.114	0.190	0.203
Mid-shaft width	0.186	0.155	0.085	-0.122	0.228	-0.176	0.152	0.078
Distal width	0.093	0.191	-0.049	-0.305	0.225	-0.086	0.186	-0.034
Height	0.118	0.090	0.262	0.422	0.221	-0.103	0.085	0.267
<b>Phalanx</b>								
Length	-0.516	0.248	-0.364	-0.040	0.185	0.532	0.262	-0.347
Proximal width	0.099	0.190	-0.028	-0.314	0.219	-0.091	0.188	-0.012
Mid-shaft width	0.265	0.157	0.150	-0.055	0.231	-0.250	0.160	0.167
Distal width	0.165	0.251	0.010	-0.136	0.227	-0.150	0.254	0.036
Height	0.141	0.187	0.308	0.469	0.221	-0.129	0.188	0.300
Digit length	-0.342	0.423	-0.277	0.297	0.198	0.355	0.421	-0.289
Eigen	2.62E-05	1.24E-05	6.91E-06	5.79E-06	7.3E-04	2.2E-05	1.1E-05	6.0E-06
% var	30.12%	14.28%	7.94%	6.64%	90.25%	2.72%	1.36%	0.75%

Note: The first four pPC loadings from shape and raw pPCAs are listed. Raw pPC1 loadings are all negative and are here multiplied by -1 to facilitate interpretation.

and flying taxa), with aerial species exhibiting the lowest morphological diversity, followed by aquatic and semi-aerial taxa (Figure 4). Species using terrestrial and semi-aquatic media are the most disparate ones. Similar patterns were detected when examining each bone separately (Figure 4b–e, Table S13). Pinnipeds also show the lowest disparity for absolute forelimb size, and bats show the smallest disparity in the absolute humerus and radius values (Figure S8, Table S14).

### 3.3 | Locomotor environment and phenotypic convergence

We detected significant forelimb shape convergence among semi-aerial mammals ( $\theta=45.62^\circ$ ,  $p=0.001$ , Table 2), as well as between aerial and semi-aerial mammals, but at a wide  $\theta$  value ( $\theta=64.64^\circ$ ,  $p=0.001$ ). The pattern of phenotypic convergence detected for the global limb shape was confirmed when examining each bone

separately, except for the metacarpal of semi-aerial and aerial groups ( $\theta=108.55^\circ$ ,  $p=0.180$ ). We did not detect shape convergence within aquatic, semi-aquatic nor between aquatic and semi-aquatic taxa—neither for whole forelimb morphology, nor for the individual bones. Without size correction, however, phenotypic convergence of the whole forelimb size is strongly detected within aquatic taxa, displaying a very narrow angle of morphospace convergence, smaller than expected by chance ( $\theta=11.05^\circ$ ,  $p=0.001$ , Table 2). Convergence in the absolute forelimb size was also detected between aerial and semi-aerial taxa, but at larger angles ( $\theta=64.80^\circ$ ,  $p=0.01$ ), and the same patterns are recovered for individual bones (Table 2).

## 4 | DISCUSSION

Solids, water and air compose the surrounding world for living organisms. Each locomotor environment exhibits particular physical

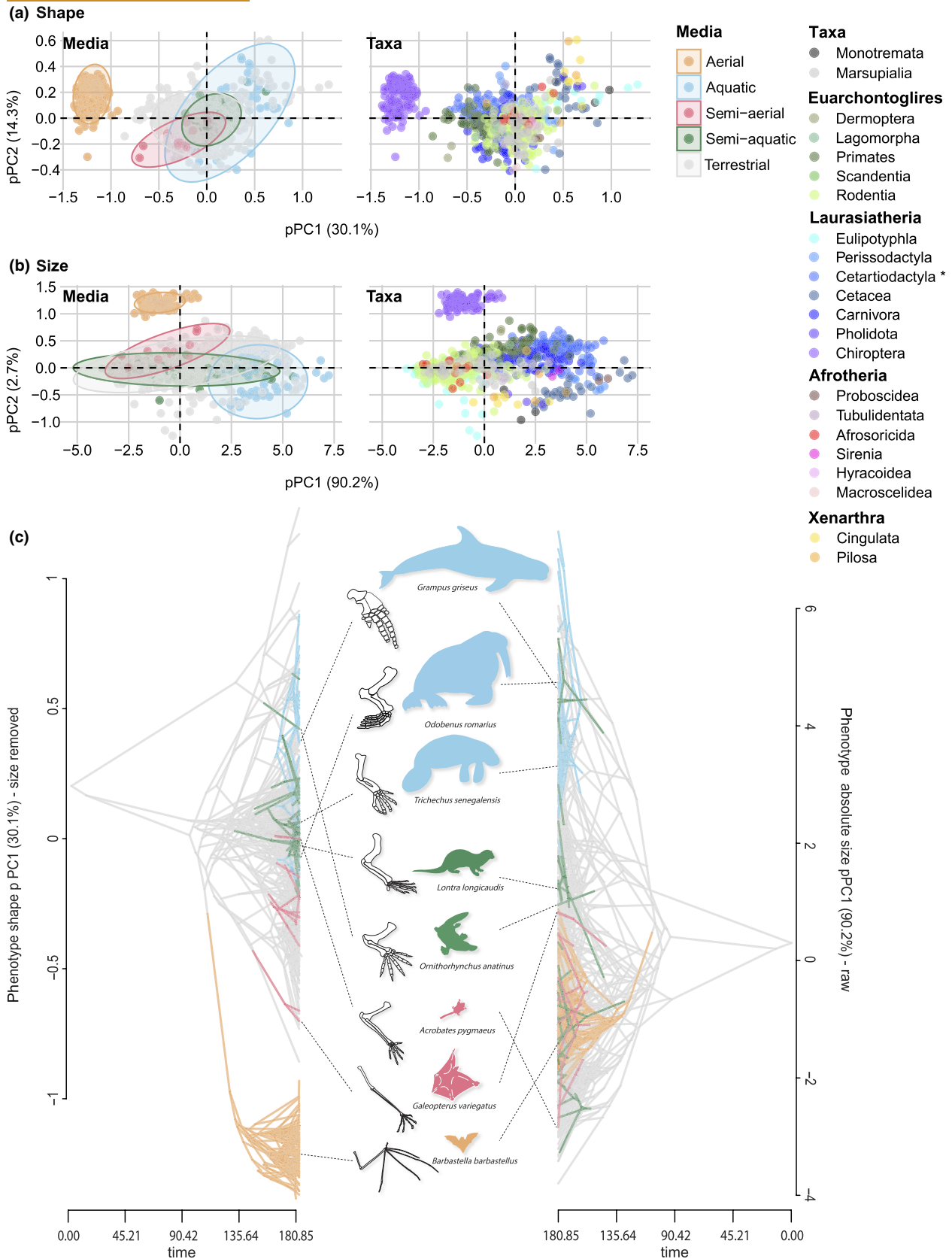


**FIGURE 2** Morphological variation of the mammalian forelimb. (a) Shape forelimb morphospaces with species coloured by locomotor medium (left) and taxonomic group (right), calculated with size residuals (ellipses indicate 95% confidence interval); (b) Absolute forelimb size morphospaces with species coloured by locomotor medium (left) and taxonomic group (right), calculated with raw data; (c) Mirrored phenograms indicating the evolutionary trajectories of the pPC1 of shape (size removed data, from 'a') and absolute size (raw data, 'b'), with coloured branches representing one possible ancestral state reconstruction of locomotor environments. Examples of species classified into non-terrestrial media are indicated (not to scale). \* Cetartiodactyla non-Cetacea.

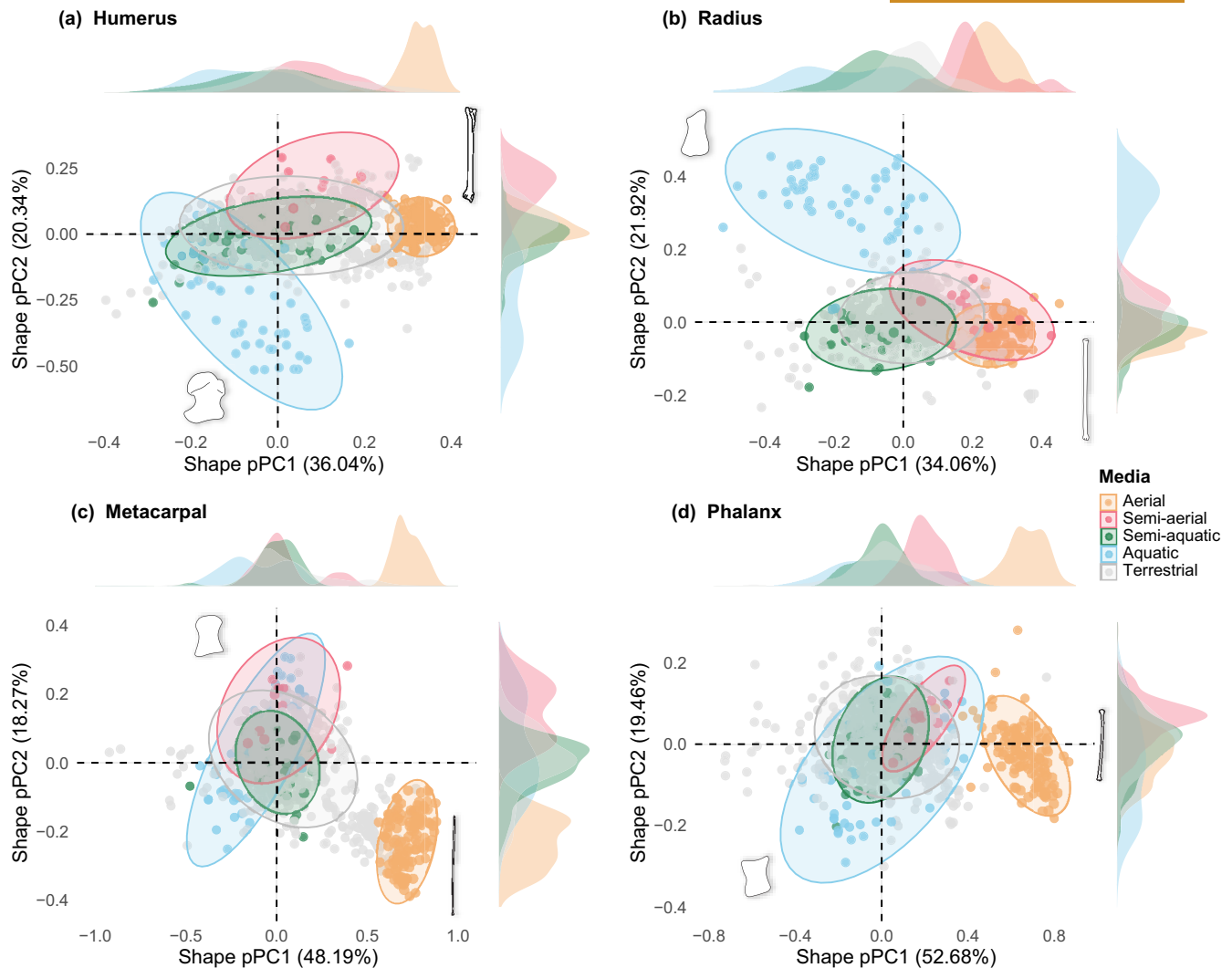


**FIGURE 3** Shape morphospace of each bone, coloured by the locomotor environment (media). Density plots on the top and right sides indicate the scores distribution per medium at each pPC. (a) Humerus, (b) radius, (c) metacarpal and (d) phalanx.

properties that constrain an animal's ability to move, potentially imposing macroevolutionary limitations on the morphological diversity of locomotor systems (Biewener & Patek, 2018). Using a dataset of forelimb measurements that represents a comprehensive coverage of the extant mammalian diversity, we show that the use of fluid media strongly explains variation in forelimb morphology. We specifically demonstrate that groups using fully aquatic habitats have the most disparate arm shapes among locomotor environment types, perhaps reflecting many-to-one mapping (Wainwright, 1996) where multiple forelimb shapes can accommodate swimming. Conversely, aerial locomotion, solely observed in bats, is associated with stronger restrictions on forelimb shape disparity which translates on partial phenotypic convergence of forelimb bones across gliding mammals and bats. Our findings indicate that locomotion in homogeneous fluids such as water and air may either facilitate or restrict morphological diversity of mammals.

The reinvasion of aquatic media by mammals is linked to a remarkable morphological diversity of overall forelimb skeletal shape. This phenomenon is also recovered for individual forelimb bone

elements (except for the metacarpal, which is more diverse in terrestrial mammals). Although all aquatic mammalian lineages must meet similar adaptive challenges to move underwater, aquatic locomotion does not constrain the skeletal evolution of the fins in mammals. Similar to the osteological shape described in this study, the external shape of the flippers (Cooper, 2009; Woodward et al., 2006), as well as their muscular anatomy (Cooper, Berta, et al., 2007), and skeletal distribution (DeBlois & Motani, 2019; Fernández et al., 2020), are quite variable across aquatic mammals, which are suggested to reflect different functional adaptations for swimming. Aquatic mammals use two general swimming strategies to provide thrust, one through the movement of the axial skeleton—exhibited by sea otters and true seals, that use undulatory pelvic movements, as well as dolphins and whales, that mostly swim through dorsoventral fluke movements—and the other through appendicular thrust provided by the limbs, observed in otariids (Biewener & Patek, 2018; Fish, 1996; Gutarra & Rahman, 2022). Consequently, the functional role of flippers varies with swimming mode (Fish, 1996; Hocking et al., 2021; Kuhn & Frey, 2012). In cetaceans, fore fins mostly function as control

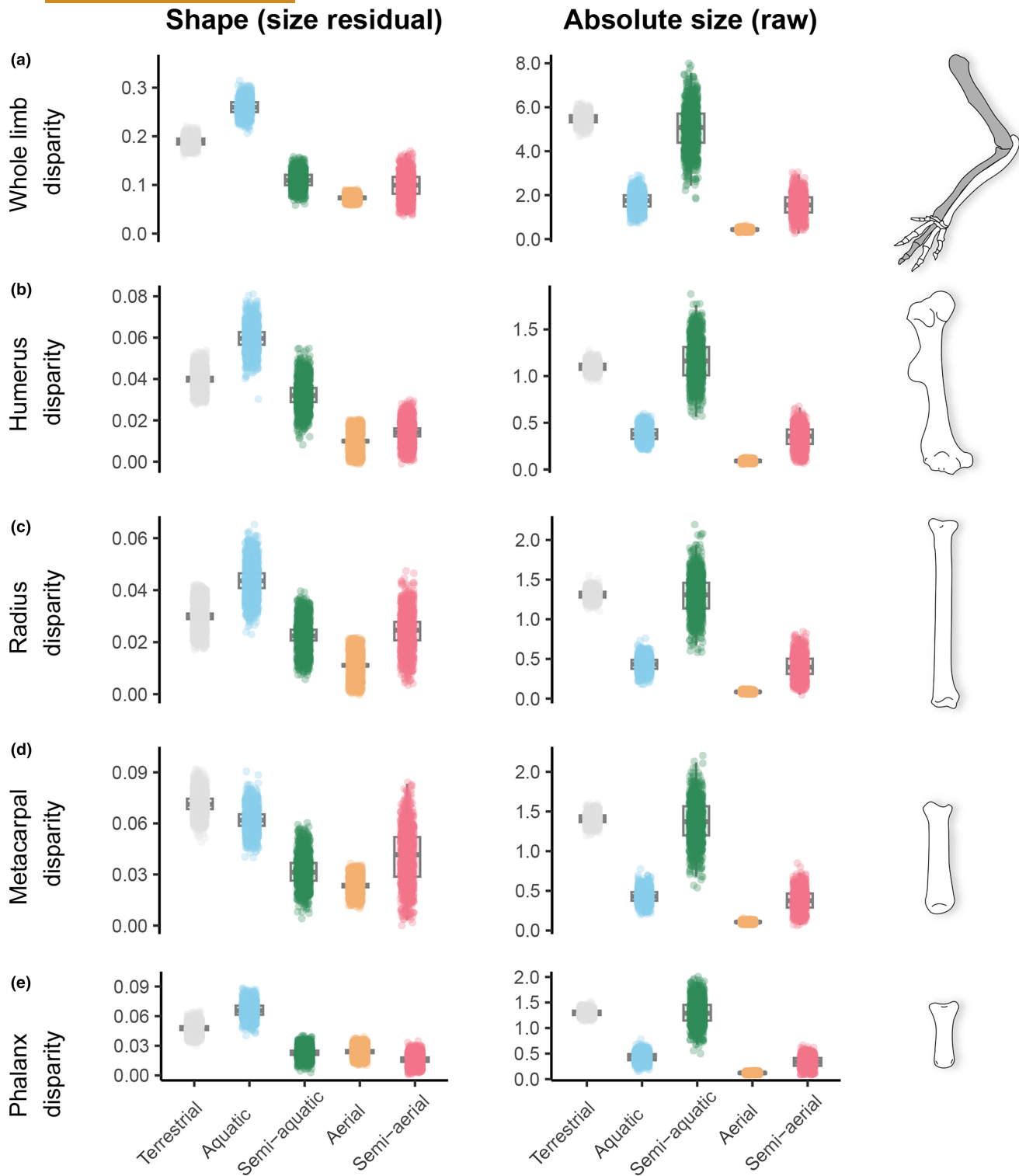


**FIGURE 4** Morphological disparity across locomotor environments (media). Left panel indicates values for trait shape (size residual), and absolute size (raw values) disparity is indicated on the right. The scatter plots with jittering represent disparity (sum of variances) calculated over 1000 bootstrap pseudoreplicates. (a) whole forelimb disparity, (b) humerus disparity, (c) radius disparity, (d) metacarpal disparity and (e) phalanx disparity.

surfaces and assist rotation and surging, with the thrust being mostly provided by the tail (Fish, 1996; Gutarra & Rahman, 2022). The flippers in this group possess a stiffened structure with limited within-limb flexibility (Cooper, Dawson, et al., 2007; DeBlois &

Motani, 2019). Sirenians use their paddle-like flippers to generate propulsion against the sea or riverine floor, also providing small movement corrections for swimming stability (Cooper, 2009). In sea lions, the flippers act as control surfaces in addition to propulsive

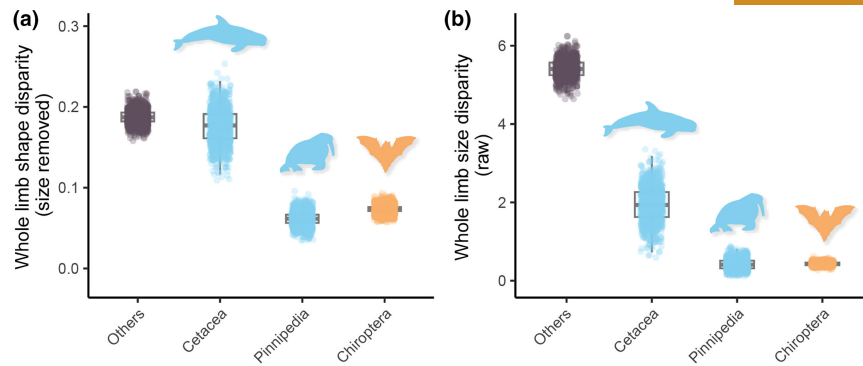


**FIGURE 5** Whole limb morphological disparity across major clades with locomotion in continuous fluid media. Studied species that do not belong to the any of the three major clades are included in 'others'. The scatter plots with jittering represent disparity (sum of variances) calculated over 1000 bootstrap pseudoreplicates. (a) Forelimb shape disparity (size residual); (b) Forelimb absolute size (raw values) disparity.

**TABLE 2** Phenotypic convergence within and between locomotor media.

State 1	State 2	Shape (size removed)		Absolute size (raw)	
		$\theta$	<i>p</i> -value	$\theta$	<i>p</i> -value
<b>Whole limb</b>					
Aquatic	—	55.82	1.000	11.05	<b>0.001</b>
Semi-aquatic	—	84.86	0.948	90.06	0.827
Semi-aerial	—	45.62	<b>0.001</b>	71.19	0.660
Aerial	Semi-aerial	64.64	<b>0.010</b>	64.80	<b>0.010</b>
Semi-aquatic	Aquatic	87.03	0.990	98.90	1.000
<b>Humerus</b>					
Aquatic	—	47.63	1.000	9.09	<b>0.001</b>
Semi-aquatic	—	88.97	0.997	91.20	0.901
Semi-aerial	—	36.98	<b>0.001</b>	70.61	0.722
Aerial	Semi-aerial	75.10	<b>0.010</b>	45.48	<b>0.010</b>
Semi-aquatic	Aquatic	87.42	1.000	97.11	0.990
<b>Radius</b>					
Aquatic	—	36.07	1.000	8.32	<b>0.001</b>
Semi-aquatic	—	77.66	0.887	90.08	0.810
Semi-aerial	—	43.90	<b>0.001</b>	78.36	0.901
Aerial	Semi-aerial	38.06	<b>0.010</b>	53.73	<b>0.010</b>
Semi-aquatic	Aquatic	88.16	1.000	100.75	1.000
<b>Metacarpal</b>					
Aquatic	—	76.55	1.000	8.87	<b>0.001</b>
Semi-aquatic	—	91.30	0.997	90.99	0.897
Semi-aerial	—	51.27	<b>0.006</b>	71.77	0.603
Aerial	Semi-aerial	108.55	0.180	74.04	<b>0.010</b>
Semi-aquatic	Aquatic	88.71	1.000	103.72	1.000
<b>Phalanx</b>					
Aquatic	—	75.91	1.000	9.08	<b>0.001</b>
Semi-aquatic	—	90.58	0.991	90.62	0.808
Semi-aerial	—	39.60	<b>0.001</b>	62.77	0.202
Aerial	Semi-aerial	36.11	<b>0.010</b>	45.28	<b>0.010</b>
Semi-aquatic	Aquatic	90.83	0.980	104.17	1.000

Note: Angles ( $\theta$ ) and significance of phenotypic convergence (of shape and absolute size values) are indicated for the whole forelimb as well as per bone. Significant *p*-values are highlighted in bold.

thrust (Fish, 1996). This biomechanical diversity reflects the shape of the forelimb elements, as propulsive-flipper tetrapods (including otariid seals, marine turtles, and penguins) tend to have less dense and robust arm bones compared to the cetacean control flippers (DeBlois & Motani, 2019). This results in forelimbs that are more flexible and efficient at producing thrust. This diversity in swimming styles further highlights how forelimb evolution in aquatic mammals is defined by many morphological and functional solutions for underwater locomotion.

Among the two most speciose aquatic clades of mammals, cetaceans show much greater forelimb shape disparity than pinnipeds. Cetaceans also present more specialised adaptations to a fully aquatic lifestyle than pinnipeds, including fur loss and complete independence from terrestrial environments for reproduction (Vermeij & Motani, 2018). Because cetacean flippers are stiff and released from their role in body weight support, within limb proportions might be less constrained, in turn contributing to the outstanding skeletal variation of this structure. Remarkably, digit length is highly variable in cetaceans (as shown by the wide pPC2 whole forelimb shape score ranges), ranging from multiple elongated phalanges (for example, the humpback whale *Megaptera novaeanglia*) to small phalanges encased by large interphalangeal joints (as observed in the killer whale *Orcinus orca*). Such variation in digit length is also reflective of the repeated evolution of hyperphalangy observed in Cetacea (Cooper, Berta, et al., 2007), which is absent in other mammalian clades. By contrast, pinnipeds spend a considerable proportion of their lives on land, even though long-distance locomotion on land is quite limited and inefficient (Kuhn & Frey, 2012). As revealed by a kinematic study using a sea turtle flipper-inspired robot, more flexible wrists are more efficient for locomotion on land than fixed joints (Mazouchova et al., 2013). Compared to cetaceans, pinniped wrists are relatively flexible, potentially due to constraints resulting from terrestrial locomotion that are not present for the stiffer and more morphologically diverse cetacean flipper.

Although forelimb shape disparity is elevated in aquatic mammals, absolute limb size variation in this group is particularly low. This is evidenced by the strong phenotypic convergence of absolute forelimb size across aquatic taxa, that is when body size was not removed from the raw data. This pattern is primarily due to the direct correlation between absolute forelimb size and body mass: aquatic mammals are on average the heaviest and largest species examined, displaying likewise large forelimbs. The evolution of such large body sizes is recurrent in aquatic tetrapods (Burin et al., 2023; Pyenson & Vermeij, 2016; Wolff & Guthrie, 1985) and, in aquatic mammals, body mass likely evolved towards a similarly high adaptive peak, which is considerably more constrained than for their terrestrial relatives (Gearty et al., 2018). Therefore, the strong evolutionary convergence detected for absolute forelimb size in groups that move underwater ultimately reflects the low disparity in their body size.

Forelimb shape in mammals that use air for locomotion is relatively more constrained than in aquatic taxa. Forelimb elongation is a shared trait among all flying tetrapods, that is bats, birds and pterosaurs, implying that the acquisition of aerial locomotion

imposes similar constraints on the evolution of body shape across vertebrates (Maher et al., 2022). In mammals, bats are the only mammal group capable of powered flight and are included in our dataset as the single representative of strict aerial locomotion. The phenotypic disparity of bat wings is low in terms of size and shape, and comparable to the disparity observed for pinnipeds, which may reflect the monophyletic origin of these groups. Yet, when compared to pterosaurs and birds, bats also have the least disparate wing shape among flying tetrapods, occupying a restricted morphospace of limb bone proportions (Gatesy & Middleton, 2007). Low skeletal disparity is consistent with the hypothesis that wing morphology reached a constrained adaptive optimum for flight in mammals. Except for the metacarpal, we observed that most of the forelimb bones in bats and gliding mammals present wide but significant convergence angles in the morphospace. Our findings are consistent with previous descriptions of incomplete convergence of the postcranial skeleton among gliding mammals, which showed that gliding adaptations are linked to the lengthening of proximal long bones (Grossnickle et al., 2020). Such elongation of the forelimb bones allows an increase in the surface area of the attached patagium, favouring air manoeuvrability and lift control (Gatesy & Middleton, 2007; Grossnickle et al., 2020). The similarities detected between bats and gliding mammals support a gliding ancestor in Chiroptera, with volant animals exhibiting intermediate morphologies between arboreal mammals and bats (Burtner et al., 2024).

Locomotion on land and at the interface of water and land characterises the groups occupying the center of the morphospace. For the absolute limb size, that is when size is not deducted from trait values, phenotypic disparity is the highest among these groups, with species using solid substrates also having the second most diverse forelimb shapes after aquatic taxa. These patterns are not surprising considering that taxa utilising terrestrial media encompass groups that use many different types of micro-habitats and display a wide variety of locomotory modes. Semi-aquatic taxa, for instance, present a more generalist locomotor apparatus capable of moving across both terrestrial and aquatic substrates and often showing intermediate and less constrained biomechanical specialisations for movement on both land and in water (Botton-Divet et al., 2017; Gutarra & Rahman, 2022; Hood, 2020). Besides demonstrating relatively high disparity, semi-aquatic taxa do not exhibit phenotypic convergence of the forelimb, which may reflect the many different degrees of adaptation to aquatic environments and the different modes used to swim (Motani & Vermeij, 2021). For example, the muskrat *Ondatra* uses pelvic paddling during swimming with limbs oriented in the vertical parasagittal plane, whereas platypuses execute mostly pectoral rowing, with limbs positioned horizontal to the body plane (Fish, 1993, 1996). Otters, use both pelvic paddling and body undulation for propulsion (Fish, 1993), illustrating the diversity of locomotor modes in these mammals.

The high disparity among terrestrial clades is due to the combination of a myriad of locomotor modes in animals that are capable of moving on land, and the grouping of multiple clades with unique

evolutionary histories and diverse body plans. Among terrestrial modes of locomotion, a great heterogeneity of forelimb bone morphology is observed for small to medium-sized mammals, particularly related to constraints for fossoriality and arboreality (Chen & Wilson, 2015; Fabre et al., 2015; Hedrick et al., 2020; Weaver & Grossnickle, 2020; Weisbecker & Schmid, 2007; Weisbecker & Warton, 2006). Mammals with fossorial habits move in dense substrates that are typically very heterogenous. Fossoriality and semi-fossoriality in many lineages has resulted in the evolution of bulky, short proximal bones and robust autopods (Chen & Wilson, 2015; Fabre et al., 2015; Hedrick et al., 2020; Nevo, 1979, 1995). Despite such similarities, fossorial mammals seem to display many morphological solutions in their limbs to deal with the biomechanical constraints for living underground (Montoya-Sanhueza et al., 2022; Sansalone et al., 2020). Conversely, arboreality seems to drive the convergent evolution of more gracile limb bones and slender phalanges, a pattern consistently observed for many mammalian lineages (Chen & Wilson, 2015; Fabre et al., 2015; Weisbecker & Schmid, 2007; Weisbecker & Warton, 2006). Although some studies have started to transpose these associations from the lineage level comparison to a higher macroevolutionary context (Maher et al., 2022), further investigation is necessary to understand how morphological evolution across distant taxa responds to similar ecological drivers.

## 5 | CONCLUSIONS

We here describe the relationships of forelimb morphological diversity and locomotor environment based on a taxonomically comprehensive dataset of mammals. We demonstrate that leaving terrestrial substrates contributed to the diversification of mammalian forelimb morphology into new regions of morphospace. Although air and water are both fluid media, they generate different constraints on forelimb evolution. Aquatic locomotion resulted in the diversification of forelimb shape, which may reflect the many functional roles of the pectoral limb while swimming. Conversely, aerial locomotion imposes more strict constraints on forelimb shape, with bats and gliding mammals exhibiting patterns of convergence mostly involving the elongation of the proximal limb segments (Burtner et al., 2024; Grossnickle et al., 2020). We show that the outstanding forelimb diversity in mammals is uneven according to the physical properties of the locomotor environment, as well as to the role it plays during locomotion, highlighting the importance of this trait in the evolutionary radiation of mammals. Overall, we demonstrate that not all locomotor environments can be traversed with the same forelimb morphology and that the locomotor environment has driven much of the morphological and functional evolution of the mammalian limb during the Cenozoic.

### AUTHOR CONTRIBUTIONS

Conceptualization: PSR, A-CF and AH; data curation: PSR, RBJB, QM, and P-HF; data acquisition: PSR; methodology: PSR, A-CF and

AH; analyses design: PSR; result interpretation: PSR, A-CF, BPH and AH; writing original draft: PSR. All authors reviewed and contributed critically to the drafts and gave final approval for publication.

### ACKNOWLEDGEMENTS

We thank the following collection managers for their support during data acquisition: at the MNHN, Alexander Nasole, Aude Lalis, Aurélie Verguin, Céline Bens, Géraldine Veron, Jacques Cuisin, Joséphine Lesur and Violaine Colin; at the AMNH, Eleanor Hoeger, Marisa Surovy and Sara Ketelsen; at the NHM, Roberto Portela and Richard Sabin. We thank Renaud Lebrun for assisting with the CT scanning. We also thank Silvia Castiglione and Julien Clavel for the assistance with their R packages. Funding was provided by the Conselho Nacional de Desenvolvimento Científico e Tecnológico (CNPq) doctoral grant to PSR (process #204841/2018-6), the Synthesis of Systematic Resources (SYNTHESES) Project, which is financed by European Community Research Infrastructure Action (FP7: Grants GB-TAF-5737 (PHF), GB-TAF-6945 (PHF) and GB-TAF-1316 (QM) to the National History Museum London), by the Agence Nationale de la Recherche (Défi des autres savoirs, Grants DS10, ANR-17-CE02-0005 RHINOGRAD 2017, PHF) and by the European Research Council (ERC-2015-STG-677774, TEMPO Mammals project to RBJB). Creation of datasets accessed on MorphoSource was made possible by the following funders and grant numbers: National Science Foundation (NSF) DBI-1701713, 1701714, 1701737, 1702263, 1701665, 1701767, 1701769, 1701870, 1701797, 701851, 1702442, 1902105, 1902242, DEB-9873663, BCS 1317525, BCS 1540421, BCS 1552848 and Leakey Foundation. Project funding for digital acquisition of each used specimen is detailed in [Supporting Information 1](#). We also acknowledge Anjali Goswami, Helder Gomes Rodrigues, Eric Guilbert, Bruno Frédérick, Geraldine Veron, John Nyakatura, Raphaël Cornette, and Sharlene Santana for their insightful comments during the elaboration of this study.

### CONFLICT OF INTEREST STATEMENT

The authors declare no conflict of interests. Anthony Herrel is an Associate Editor of *Functional Ecology* but took no part in the editorial process.

### DATA AVAILABILITY STATEMENT

Data and codes are available on GitHub: [https://github.com/psrot hier/of\\_flippers\\_and\\_wings-FuncEcol](https://github.com/psrot hier/of_flippers_and_wings-FuncEcol). And archived on Zenodo: <https://doi.org/10.5281/zenodo.13144111>.

### STATEMENT OF INCLUSION

Our study examines the morphological variation of mammals from all around the globe, combining secondary digital data from online repositories with multiple specimens provided by different zoological collections. As such, there was no concentration of local data collection. The geographical distribution of the authorship team represents major regions of interest in the analysis. Whenever relevant, literature published by scientists from the regions not represented by the authorship was also cited.

## ORCID

Priscilla S. Rothier  <https://orcid.org/0000-0003-3017-6528>  
 Anne-Claire Fabre  <https://orcid.org/0000-0001-7310-1775>  
 Roger B. J. Benson  <https://orcid.org/0000-0001-8244-6177>  
 Quentin Martinez  <https://orcid.org/0000-0002-7127-4012>  
 Pierre-Henri Fabre  <https://orcid.org/0000-0002-3414-5625>  
 Brandon P. Hedrick  <https://orcid.org/0000-0003-4446-3405>  
 Anthony Herrel  <https://orcid.org/0000-0003-0991-4434>

## REFERENCES

- Benson, R. B. J., Hunt, G., Carrano, M. T., & Campione, N. (2018). Cope's rule and the adaptive landscape of dinosaur body size evolution. *Palaeontology*, 61(1), 13–48. <https://doi.org/10.1111/pala.12329>
- Biewener, A. A., & Patek, S. N. (2018). *Animal locomotion* (2nd ed.). Oxford University Press.
- Bishop, K. L. (2008). The evolution of flight in bats: Narrowing the field of plausible hypothesis. *The Quaternary Review of Biology*, 83(2), 153–169. <https://doi.org/10.1086/587825>
- Botton-Divet, L., Cornette, R., Houssaye, A., Fabre, A.-C., & Herrel, A. (2017). Swimming and running: A study of the convergence in long bone morphology among semi-aquatic mustelids (Carnivora: Mustelidae). *Biological Journal of the Linnean Society*, 121, 38–49. <https://doi.org/10.1093/biolinnean/blw027>
- Burin, G., Park, T., James, T. D., Slater, G. J., & Cooper, N. (2023). The dynamic adaptive landscape of cetacean body size. *Current Biology*, 33, 1787–1794.e3. <https://doi.org/10.1016/j.cub.2023.03.014>
- Burtner, A. E., Grossnickle, D. M., Santana, S. E., & Law, C. J. (2024). Gliding toward an understanding of the origin of flight in bats. *PeerJ*, 12, e17824. <https://doi.org/10.7717/peerj.17824>
- Castiglione, S., Serio, C., Tamagnini, D., Melchionna, M., Mondanaro, A., Di Febraro, M., Profico, A., Piras, P., Barattolo, F., & Raia, P. (2019). A new, fast method to search for morphological convergence with shape data. *PLoS One*, 14(12), e0226949. <https://doi.org/10.1371/journal.pone.0226949>
- Castiglione, S., Tesone, G., Piccolo, M., Melchionna, M., Mondanaro, A., Serio, C., Di Febraro, M., & Raia, P. (2018). A new method for testing evolutionary rate variation and shifts in phenotypic evolution. *Methods in Ecology and Evolution*, 9(4), 974–983. <https://doi.org/10.1111/2041-210X.12954>
- Chen, M., & Wilson, G. P. (2015). A multivariate approach to infer locomotor modes in Mesozoic mammals. *Paleobiology*, 21(2), 280–312. <https://doi.org/10.5061/dryad.870j3>
- Clavel, J., Aristide, L., & Morlon, H. (2019). A penalized likelihood framework for high-dimensional phylogenetic comparative methods and an application to new-world monkeys brain evolution. *Systematic Biology*, 68(1), 93–116. <https://doi.org/10.1093/sysbio/syy045>
- Clavel, J., Escarguel, G., & Merceron, G. (2015). mvMORPH: An R package for fitting multivariate evolutionary models to morphometric data. *Methods in Ecology and Evolution*, 6(11), 1311–1319. <https://doi.org/10.1111/2041-210X.12420>
- Clavel, J., & Morlon, H. (2020). Reliable phylogenetic regressions for multivariate comparative data: Illustration with the MANOVA and application to the effect of diet on mandible morphology in Phyllostomid bats. *Systematic Biology*, 69(5), 927–943. <https://doi.org/10.1093/sysbio/syaa010>
- Clifford, A. B. (2010). The evolution of the unguligrade manus in artiodactyls. *Journal of Vertebrate Paleontology*, 30(6), 1827–1839. <https://doi.org/10.1080/02724634.2010.521216>
- Cooper, L. N. (2009). Forelimb anatomy. In B. Würsig, J. G. M. Thewissen, & K. M. Kovacs (Eds.), *Encyclopedia of marine mammals: Vol. second edition* (pp. 449–452). Academic Press.
- Cooper, L. N., Berta, A., Dawson, S. D., & Reidenberg, J. S. (2007). Evolution of hyperphalangy and digit reduction in the cetacean manus. *Anatomical Record*, 290(6), 654–672. <https://doi.org/10.1002/ar.20532>
- Cooper, L. N., Dawson, S. D., Reidenberg, J. S., & Berta, A. (2007). Neuromuscular anatomy and evolution of the cetacean forelimb. *Anatomical Record*, 290(9), 1121–1137. <https://doi.org/10.1002/ar.20571>
- DeBlois, M. C., & Motani, R. (2019). Flipper bone distribution reveals flexible trailing edge in underwater flying marine tetrapods. *Journal of Morphology*, 280(6), 908–924. <https://doi.org/10.1002/jmor.20992>
- Dudley, R., Byrnes, G., Yanoviak, S. P., Borrell, B., Brown, R. M., & McGuire, J. A. (2007). Gliding and the functional origins of flight: Biomechanical novelty or necessity? *Annual Review of Ecology, Evolution, and Systematics*, 38, 179–201. <https://doi.org/10.1146/annurev.ecolsys.37.091305.110014>
- Fabre, A.-C., Cornette, R., Goswami, A., & Peigné, S. (2015). Do constraints associated with the locomotor habitat drive the evolution of forelimb shape? A case study in musteloid carnivores. *Journal of Anatomy*, 226(6), 596–610. <https://doi.org/10.1111/joa.12315>
- Fernández, M. S., Vlachos, E., Buono, M. R., Alzugaray, L., Campos, L., Sterli, J., Herrera, Y., & Paolucci, F. (2020). Fingers zipped up or baby mittens? Two main tetrapod strategies to return to the sea. *Biology Letters*, 16(8), 20200281. <https://doi.org/10.1098/rsbl.2020.0281>
- Fish, F. E. (1993). Influence of hydrodynamic design and propulsive mode on mammalian swimming energetics. *Australian Journal of Zoology*, 42, 79–101. <https://doi.org/10.1071/ZO9940079>
- Fish, F. E. (1996). Transitions from drag-based to lift-based propulsion in mammalian swimming. *American Zoologist*, 36(6), 628–641. <https://doi.org/10.1093/icb/36.6.628>
- Fish, F. E., Howle, L. E., & Murray, M. M. (2008). Hydrodynamic flow control in marine mammals. *Integrative and Comparative Biology*, 48(6), 788–800. <https://doi.org/10.1093/icb/icn029>
- Gatesy, S. M., & Middleton, K. M. (2007). Skeletal adaptations for flight. In B. K. Hall (Ed.), *Fins into limbs: Evolution, development, and transformation* (pp. 269–283). The University of Chicago Press.
- Gearty, W., McClain, C. R., & Payne, J. L. (2018). Energetic tradeoffs control the size distribution of aquatic mammals. *Proceedings of the National Academy of Sciences of the United States of America*, 115(16), 4194–4199. <https://doi.org/10.1073/pnas.1712629115>
- Godoy, P. L., Benson, R. B. J., Bronzati, M., & Butler, R. J. (2019). The multi-peak adaptive landscape of crocodylomorph body size evolution. *BMC Evolutionary Biology*, 19(1), 167. <https://doi.org/10.1186/s12862-019-1466-4>
- Grossnickle, D. M., Chen, M., Wauer, J. G. A., Pevsner, S. K., Weaver, L. N., Meng, Q. J., Liu, D., Zhang, Y. G., & Luo, Z. X. (2020). Incomplete convergence of gliding mammal skeletons. *Evolution*, 74(12), 2662–2680. <https://doi.org/10.1111/evo.14094>
- Guillerme, T. (2018). dispRity: A modular R package for measuring disparity. *Methods in Ecology and Evolution*, 9(7), 1755–1763. <https://doi.org/10.1111/2041-210X.13022>
- Guillerme, T., Cooper, N., Brusatte, S. L., Davis, K. E., Jackson, A. L., Gerber, S., Goswami, A., Healy, K., Hopkins, M. J., Jones, M. E. H., Lloyd, G. T., O'Reilly, J. E., Pate, A., Puttick, M. N., Rayfield, E. J., Saupe, E. E., Sherratt, E., Slater, G. J., Weisbecker, V., ... Donoghue, P. C. J. (2020). Disparities in the analysis of morphological disparity. *Biology Letters*, 16(7), 20200199. <https://doi.org/10.1098/rsbl.2020.0199>
- Gutarra, S., & Rahman, I. A. (2022). The locomotion of extinct secondarily aquatic tetrapods. *Biological Reviews*, 97(1), 67–98. <https://doi.org/10.1111/brv.12790>
- Gutarra, S., Stubbs, T. L., Moon, B. C., Palmer, C., & Benton, M. J. (2022). Large size in aquatic tetrapods compensates for high drag caused by extreme body proportions. *Communications Biology*, 5(1), 380. <https://doi.org/10.1038/s42003-022-03322-y>
- Harmon, L. J., Losos, J. B., Jonathan Davies, T., Gillespie, R. G., Gittleman, J. L., Bryan Jennings, W., Kozak, K. H., McPeck, M. A., Moreno-Roark, F., Near, T. J., Purvis, A., Ricklefs, R. E., Schluter, D., Schulte,

- J. A., Seehausen, O., Sidlauskas, B. L., Torres-Carvajal, O., Weir, J. T., & Mooers, A. T. (2010). Early bursts of body size and shape evolution are rare in comparative data. *Evolution*, 64(8), 2385–2396. <https://doi.org/10.1111/j.1558-5646.2010.01025.x>
- Hedrick, B. P., Dickson, B. V., Dumont, E. R., & Pierce, S. E. (2020). The evolutionary diversity of locomotor innovation in rodents is not linked to proximal limb morphology. *Scientific Reports*, 10(1), 717. <https://doi.org/10.1038/s41598-019-57144-w>
- Hocking, D. P., Marx, F. G., Wang, S., Burton, D., Thompson, M., Park, T., Burville, B., Richards, H. L., Sattler, R., Robbins, J., Miguez, R. P., Fitzgerald, E. M. G., Slip, D. J., & Evans, A. R. (2021). Convergent evolution of forelimb-propelled swimming in seals. *Current Biology*, 31(11), 2404–2409.e2. <https://doi.org/10.1016/j.cub.2021.03.019>
- Hood, G. A. (2020). *Semi-aquatic mammals: Ecology and biology*. John Hopkins University Press.
- Howell, A. B. (1970). *Aquatic mammals: Their adaptations to life in the water*. Dover Publication Inc.
- Jackson, S. M. (2000). Glide angle in the genus *Petaurus* and a review of gliding in mammals. *Mammal Review*, 30(1), 9–30. <https://doi.org/10.1046/j.1365-2907.2000.00056.x>
- Jones, K. E., Bielby, J., Cardillo, M., Fritz, S. A., O'Dell, J., David, C., Orme, L., Safi, K., Sechrest, W., Boakes, E. H., Carbone, C., Connolly, C., Cutts, M. J., Foster, J. K., Grenyer, R., Habib, M., Plaster, C. A., Price, S. A., Rigby, E. A., ... Purvis, A. (2009). PanTHERIA: A species-level database of life history, ecology, and geography of extant and recently extinct mammals. *Ecology*, 90(9), 2648. <https://doi.org/10.1890/08-1494.1>
- Kiat, Y., Slavenko, A., & Sapir, N. (2021). Body mass and geographic distribution determined the evolution of the wing flight-feather molt strategy in the Neornithes lineage. *Scientific Reports*, 11(1), 21573. <https://doi.org/10.1038/s41598-021-00964-6>
- Kuhn, C., & Frey, E. (2012). Walking like caterpillars, flying like bats-pinniped locomotion. *Palaeobiodiversity and Palaeoenvironments*, 92(2), 197–210. <https://doi.org/10.1007/s12549-012-0077-5>
- Maher, A. E., Burin, G., Cox, P. G., Maddox, T. W., Maidment, S. C. R., Cooper, N., Schachner, E. R., & Bates, K. T. (2022). Body size, shape and ecology in tetrapods. *Nature Communications*, 13(1), 4340. <https://doi.org/10.1038/s41467-022-32028-2>
- Mammal Diversity Database. (2023). Mammal diversity database (version 1.11). [Data Set]. *Zenodo*. <https://doi.org/10.5281/zenodo.7830771>
- Mazouchova, N., Umbanhowar, P. B., & Goldman, D. I. (2013). Flipper-driven terrestrial locomotion of a sea turtle-inspired robot. *Bioinspiration & Biomimetics*, 8(2), 026007. <https://doi.org/10.1088/1748-3182/8/2/026007>
- McHorse, B. K., Biewener, A. A., & Pierce, S. E. (2019). The evolution of a single toe in horses: Causes, consequences, and the way forward. *Integrative and Comparative Biology*, 59(3), 638–655. <https://doi.org/10.1093/icb/icz050>
- Montoya-Sanhueza, G., Šaffa, G., Šumbera, R., Chinsamy, A., Jarvis, J. U. M., & Bennett, N. C. (2022). Fossorial adaptations in African mole-rats (Bathyergidae) and the unique appendicular phenotype of naked mole-rats. *Communications Biology*, 5(1), 526. <https://doi.org/10.1038/s42003-022-03480-z>
- Motani, R., & Vermeij, G. J. (2021). Ecophysiological steps of marine adaptation in extant and extinct non-avian tetrapods. *Biological Reviews*, 96(5), 1769–1798. <https://doi.org/10.1111/brv.12724>
- Nevo, E. (1979). Adaptive convergence and divergence of subterranean mammals. *Annual Review of Ecology and Systematics*, 10, 269–308. <https://doi.org/10.1146/annurev.es.10.110179.001413>
- Nevo, E. (1995). Mammalian evolution underground. The ecological-genetic-phenetic interfaces. *Acta Theriologica*, 3, 9–31. <https://doi.org/10.4098/AT.ARCH.95-43>
- Norberg, U. M. (1985). Evolution of vertebrate flight: An aerodynamic model for the transition from gliding to active flight. *The American Naturalist*, 126(3), 303–327. <https://doi.org/10.1086/284419>
- Nowak, R. M. (1999). *Walker's mammals of the world*. Johns Hopkins University Press.
- Polly, D. (2007). Limbs in mammalian evolution. In B. K. Hall (Ed.), *Fins into limbs: Evolution, development, and transformation* (pp. 245–268). The University of Chicago Press.
- Prothero, D. R. (2009). Evolutionary transitions in the fossil record of terrestrial hoofed mammals. *Evolution: Education and Outreach*, 2(2), 289–302. <https://doi.org/10.1007/s12052-009-0136-1>
- Pyenson, N. D., & Vermeij, G. J. (2016). The rise of ocean giants: Maximum body size in Cenozoic marine mammals as an indicator for productivity in the Pacific and Atlantic oceans. *Biology Letters*, 12(7), 20160186. <https://doi.org/10.1098/rsbl.2016.0186>
- R Core Team. (2023). *R: A language and environment for statistical computing*. R Foundation for Statistical Computing. <https://www.R-project.org/>
- Rayner, J. M. V. (1988). The evolution of vertebrate flight. *Biological Journal of the Linnean Society*, 34(3), 269–287. <https://doi.org/10.1111/j.1095-8312.1988.tb01963.x>
- Revell, L. J. (2009). Size-correction and principal components for interspecific comparative studies. *Evolution*, 63(12), 3258–3268. <https://doi.org/10.1111/j.1558-5646.2009.00804.x>
- Revell, L. J. (2012). phytools: An R package for phylogenetic comparative biology (and other things). *Methods in Ecology and Evolution*, 3(2), 217–223. <https://doi.org/10.1111/j.2041-210X.2011.00169.x>
- Rothier, P. S., Fabre, A.-C., Clavel, J., Benson, R. B. J., & Herrel, A. (2023). Mammalian forelimb evolution is driven by uneven proximal-to-distal morphological diversity. *eLife*, 12, e81492. <https://doi.org/10.7554/eLife.81492>
- Sansalone, G., Castiglione, S., Raia, P., Archer, M., Dickson, B., Hand, S., Piras, P., Profico, A., & Wroe, S. (2020). Decoupling functional and morphological convergence, the study case of fossorial Mammalia. *Frontiers in Earth Science*, 8, 112. <https://doi.org/10.3389/feart.2020.00112>
- Schliep, K. P. (2011). phangorn: Phylogenetic analysis in R. *Bioinformatics*, 27(4), 592–593. <https://doi.org/10.1093/bioinformatics/btq706>
- Sears, K., Behringer, R. R., Rasweiler, J. J., & Niswander, L. A. (2007). The evolutionary and developmental basis of parallel reduction in mammalian zeugopod elements. *The American Naturalist*, 169(1), 105–117. <https://doi.org/10.1086/510259>
- Shubin, N., Tabin, C., & Carroll, S. (1997). Fossils, genes and the evolution of animal limbs. *Nature*, 388, 639–648. <https://doi.org/10.1038/41710>
- Smith, F. A., & Lyons, S. K. (2011). How big should a mammal be? A macroecological look at mammalian body size over space and time. *Philosophical Transactions of the Royal Society, B: Biological Sciences*, 366(1576), 2364–2378. <https://doi.org/10.1098/rstb.2011.0067>
- Upham, N. S., Esselstyn, J. A., & Jetz, W. (2019). Inferring the mammal tree: Species-level sets of phylogenies for questions in ecology, evolution, and conservation. *PLoS Biology*, 17(12), e3000494. <https://doi.org/10.1371/journal.pbio.3000494>
- Vermeij, G. J., & Motani, R. (2018). Land to sea transitions in vertebrates: The dynamics of colonization. *Paleobiology*, 44(2), 237–250. <https://doi.org/10.1017/pab.2017.37>
- Vogel, S. (2020). *Life in moving fluids: The physical biology of flow-revised and expanded* (2nd ed.). Princeton University Press.
- Wainwright, P. C. (1996). Ecological explanation through functional morphology: The feeding biology of sunfishes. *Ecology*, 77(5), 1336–1343.
- Weaver, L. N., & Grossnickle, D. M. (2020). Functional diversity of small-mammal postcrania is linked to both substrate preference and body size. *Current Zoology*, 66(5), 539–553. <https://doi.org/10.1093/cz/zoaa057>
- Weisbecker, V., & Schmid, S. (2007). Autopodial skeletal diversity in hystricognath rodents: Functional and phylogenetic aspects. *Mammalian Biology*, 72(1), 27–44. <https://doi.org/10.1016/j.mam-bio.2006.03.005>

- Weisbecker, V., & Warton, D. I. (2006). Evidence at hand: Diversity, functional implications, and locomotor prediction in intrinsic hand proportions of diprotodontian marsupials. *Journal of Morphology*, 267(12), 1469–1485. <https://doi.org/10.1002/jmor.10495>
- Wolff, J. O., & Guthrie, R. D. (1985). Why are aquatic small mammals so large? *Oikos*, 45(3), 365–373. <https://doi.org/10.2307/3565572>
- Woodward, B. L., Winn, J. P., & Fish, F. E. (2006). Morphological specializations of baleen whales associated with hydrodynamic performance and ecological niche. *Journal of Morphology*, 267(11), 1284–1294. <https://doi.org/10.1002/jmor.10474>

## SUPPORTING INFORMATION

Additional supporting information can be found online in the Supporting Information section at the end of this article.

**Figure S1.** Whole limb morphospace.

**Figure S2.** Humerus morphospace.

**Figure S3.** Radius morphospace.

**Figure S4.** Metacarpal morphospace.

**Figure S5.** Phalanx morphospace.

**Figure S6.** Rarefaction curves and disparity (sum of variances) across ecological datasets.

**Figure S7.** Rarefaction curves and disparity (sum of variances) across group comparison (Chiroptera, Cetacea, Pinnipedia, and all other taxa).

**Figure S8.** Limb bone disparity in major monophyletic taxa with continuous media-based locomotion.

**Table S1.** Analyzed specimens.

**Table S2.** Description of morphometric data.

**Table S3.** Fits of linear models of evolution for the whole limb and for each bone separately.

**Table S4.** *p*-values from phylogenetic generalized least squares regressions.

**Table S5.** Whole limb principal components loadings from ordinary PCA.

**Table S6.** Phylogenetic principal component loadings for each bone measured.

**Table S7.** Principal components loadings from ordinary PCA of each bone.

**Table S8.** Whole limb morphological similarity (P-values) between locomotor medium.

**Table S9.** Humerus morphological similarity (P-values) between locomotor medium.

**Table S10.** Radius morphological similarity (P-values) between locomotor medium.

**Table S11.** Metacarpal morphological similarity (P-values) between locomotor medium.

**Table S12.** Phalanx morphological similarity (P-values) between locomotor medium.

**Table S13.** Limb disparity across locomotor media.

**Table S14.** Limb disparity across major clades using homogeneous fluid medium.

**How to cite this article:** Rothier, P. S., Fabre, A.-C., Benson, R. B. J., Martinez, Q., Fabre, P.-H., Hedrick, B. P., & Herrel, A. (2024). Of flippers and wings: The locomotor environment as a driver of the evolution of forelimb morphological diversity in mammals. *Functional Ecology*, 00, 1–16. <https://doi.org/10.1111/1365-2435.14632>